Seismic response of rocking bridge bents with parameterized flag-shaped hysteretic behaviour

A.I. Giouvanidis, & E.G. Dimitrakopoulos

Department of Civil & Environmental Engineering, The Hong Kong University of Science & Technology, Kowloon Bay, Hong Kong.

M.J. DeJong

Department of Engineering, University of Cambridge, Trumpington Street, Cambridge, UK.

ABSTRACT: The present work investigates the seismic performance of a rocking bridge bent, which is either freestanding or hybrid (supplemented with energy dissipation and re-centering devices), exhibiting flag-shaped hysteretic behaviour. Such hybrid systems have been proposed by several researchers as high-performance systems that can survive major earthquakes without substantial damage. This study considers three different structural rocking systems with either negative, zero, or positive lateral stiffness and compares their seismic performance with the pertinent freestanding structure. Both pulse-type and non-pulse-type ground motions are considered. The analysis demonstrates performance enhancement as the stiffness of the system increases and as the size of the columns decreases. However, this improvement is marginal among the examined stiffness systems. Further, it is shown that depending on the characteristics of the examined earthquake record, a different rocking design solution (e.g. freestanding, hybrid with negative/zero/positive stiffness) might exhibit better seismic behaviour.

1 INTRODUCTION

Rocking, as a means of seismic isolation, is attracting the interest of many researchers for almost a century (Kirkpatrick 1927, Housner 1963, Yim et al. 1980). Of particular interest for bridge engineering is the rocking frame configuration of Fig. 1 proposed by Mander and Cheng (1997) as a "damage avoidance design" for bridges. Makris and Vassiliou (2012) and DeJong and Dimitrakopoulos (2014) revisited the seismic response of the freestanding rocking frame. The former study revealed that the stability of the frame increases the more top-heavy it is. Soon after, Makris and Vassiliou (2014) studied a rocking frame enhanced with elastic prestressed central tendons and showed that the effect of the tendons becomes immaterial as the size of the columns or the weight of the cap-beam increases.

The development of self-centering systems aims to eliminate residual drifts after earthquakes. The combined use of re-centering and energy dissipation devices leads to "hybrid rocking systems" which exhibit flag shaped hysteretic behaviour (FSHB). Such systems have been proposed for both buildings (Eatherton and Hajjar 2011, Wiebe and Christopoulos 2014) and bridges (Palermo et al. 2005, Palermo et al. 2007, Pollino and Bruneau 2007, Marriott et al. 2009, Kam et al. 2010). Within this context, Dimitrakopoulos and Giouvanidis (2015) revisited the hybrid rocking frame by examining an asymmetric configuration (with columns unequal in height), and compared its stability with the pertinent symmetric configuration. That study unveiled the marginal influence of the asymmetry on the stability despite the very different kinematics between the two configurations.

While many "hybrid rocking systems" allow rocking in some fashion, the beneficial isolation effect originating from the negative stiffness may be minimal or non-existent. To this end, the present study extends previous research on the hybrid rocking frame (Kam et al. 2010, Dimitrakopoulos and Giouvanidis 2015) examining a rocking configuration (Fig. 1) whose response is controlled by supplemental re-centering and energy dissipation devices, exhibiting flag-shaped hysteretic behaviour (FSHB).

2 ANALYTICAL MODELING OF THE HYBRID ROCKING BRIDGE BENT

This section examines analytically the seismic response of a hybrid rocking bridge bent with flag-shaped hysteretic behaviour (FSHB). Consider the rocking frame of Fig. 1 enhanced with central (slack) tendons to provide additional re-centering capacity, and buckling restrained braces (BRBs) to dissipate the energy. This study assumes that the tendons remain linear elastic and the buckling restrained braces behave in a bilinear hysteretic fashion.

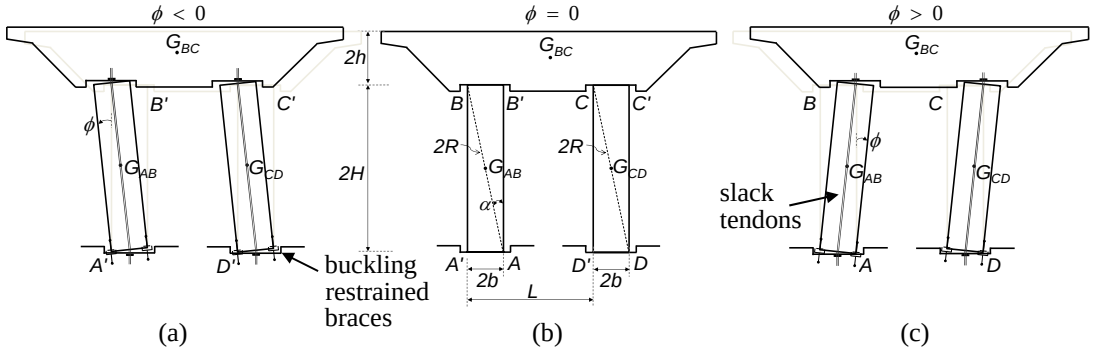

Fig. 1 The examined hybrid rocking bridge bent (a) during counter-clockwise rotation, (b) at rest position and (c) during clockwise rotation

To describe the hysteretic system the Bouc-Wen model (Bouc 1967, Wen 1976) is adopted. The restoring dissipating force is expressed as:

$$F_D = \varepsilon k_d u(t) + (1-\varepsilon) k_d u_y z(t) \tag{1}$$

where ε is the post-yield to pre-yield elastic stiffness (k_d) ratio, u_y is the yield displacement of the brace equal to $u_y = 4b\sin(\phi_y/2)$ with ϕ_y being the yield rotation and b the half base length of the column. Following Black et al. (2004), ε=0.025 and u_y=3.5mm. z is a dimensionless hysteretic parameter defined by:

$$\dot{z}(t) = \frac{1}{u_y}\left[\dot{u}(t) - \gamma|\dot{u}(t)||z|\cdot|z|^{n-1} - \beta\dot{u}(t)|z|^n\right] \tag{2}$$

Parameters β, γ and n control the shape of the hysteretic loop and for the present analysis are taken equal with 0.55, 0.45 and 1.0 respectively (Black et al. 2004).

2.1 Flag-Shaped Hysteretic Behaviour (FSHB)

During rocking, the restoring moment due to the gravitational forces of the frame assuming small rocking rotations ($\cos\phi \approx 1$, $\sin\phi \approx \phi$) and slender structures becomes:

$$\frac{M_R^{fr}}{2(m_{AB}+m_{BC})gR} = \alpha - \phi \tag{3}$$

where m_{AB} and m_{BC} are the masses of the column and the cap-beam respectively, R is the half diagonal length of the column, α is the slenderness of the column and ϕ selected to be the generalized coordinate (Fig. 1). The additional restoring moment due to the tendons and the dissipators:

$$\frac{M_R^{hyb}}{2(m_{AB}+m_{BC})gR} = 4(\rho_t + \varepsilon\rho_d)\phi + 4(1-\varepsilon)\rho_d\phi_y z(t) \tag{4}$$

The dimensionless parameters ρ_t and ρ_d control the stiffness of the tendon (k_t) and the dissipator (k_d) respectively, and are equal to:

$$\rho_t = \frac{k_t b^2}{(m_{AB}+m_{BC})gR}, \quad \rho_d = \frac{k_d b^2}{(m_{AB}+m_{BC})gR} \tag{5}$$

This study assumes that the (dimensionless) design parameters ρ_t and ρ_d vary within $0 \le \rho_t \le 0.7$ and $0 \le \rho_d \le 5.0$ respectively. The total restoring moment becomes:

$$\frac{M_R}{2(m_{AB}+m_{BC})gR} = \alpha + 4(1-\varepsilon)\rho_d \phi_y z(t) + \left[4(\rho_t + \varepsilon\rho_d) - 1\right]\phi \tag{6}$$

On the other hand, overturning is caused by the ground excitation ($\ddot{u}_g$). Hence:

$$\frac{M_{OT}}{2(m_{AB}+m_{BC})\ddot{u}_g R} = 1 + \alpha\phi \tag{7}$$

During rocking, the moment-rotation relationship (Eqs (3), (4), (6)) follow the curves in Fig. 2. Note that the restoring moment due to the gravitational forces does not enclose any area (Fig. 2(a)) since energy is dissipated only during impact with the coefficient of restitution, which connects the angular velocities after and before the impact (Dimitrakopoulos and Giouvanidis 2015):

$$\eta = \frac{\dot{\phi}^+}{\dot{\phi}^-} = \frac{1 - \frac{3}{2}\sin^2\alpha + 3\gamma_m \cos 2\alpha}{1 + 3\gamma_m} \tag{8}$$

Eq. (8) provides the maximum theoretical value of the coefficient of restitution. For the present analysis it is taken as 0.92. Energy is also dissipated due to the hysteretic behaviour of the buckling restrained braces (Fig. 2(b)). This combination leads to a flag-shaped hysteretic behaviour system (Fig. 2(c)).

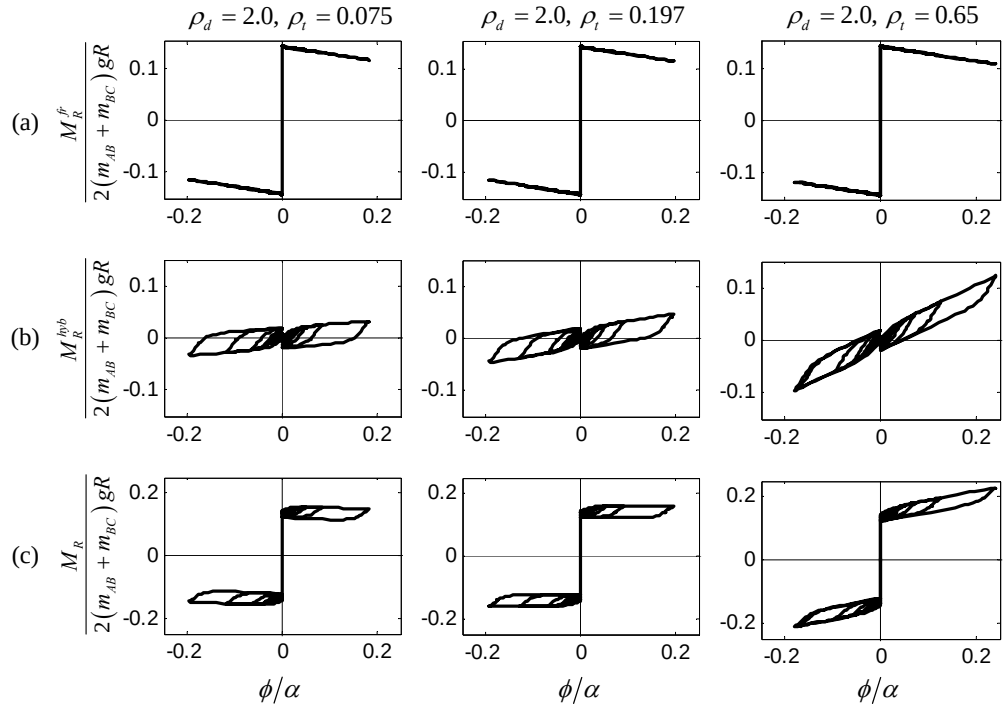

Fig. 2 Restoring moments due to (a) gravitational forces, (b) the presence of tendon and dissipator and (c) total restoring moment for the rocking frame with u_y=3.5 mm, subjected to M&P pulse (v_g=45°, γ_g=2.0, α_g=0.60g and T_g=1.03sec)

An increase in the tendon's and the dissipator's stiffness causes increase in the overall stiffness of the system, such that a transition from negative to positive lateral stiffness occurs (Fig. 2) when:

$$\rho_t + \varepsilon\rho_d > \frac{1}{4} \tag{9}$$

2.2 Equation of motion

The equation of motion of the hybrid rocking frame of Fig. 1 with flag-shaped hysteretic behaviour (FSHB) is derived from Lagrange's equation. The calculation of the kinetic (T) and the potential energy (V) of the system follows from Dimitrakopoulos and Giouvanidis (2015). The calculation of the virtual work of the non-conservative forces yields the following expression for the generalized forces.

$$Q=-4b\cos\frac{\phi}{2}\left[\varepsilon k_d u(t)+(1-\varepsilon)k_d u_y z(t)\right] \tag{10}$$

Finally, the equation which describes the rocking motion (for both signs of rotation) of the hybrid frame with flag-shaped hysteretic behaviour (FSHB) becomes:

$$\ddot{\phi}=-\frac{1+2\gamma_m}{1+3\gamma_m}p^2\begin{bmatrix}\sin\left(\alpha\,\mathrm{sgn}(\phi)-\phi\right)+\frac{\ddot{u}_g}{g}\cos\left(\alpha\,\mathrm{sgn}(\phi)-\phi\right)\\ +4\left(\rho_t+\varepsilon\rho_d\right)\sin\phi+8(1-\varepsilon)\rho_d\sin\frac{\phi_y}{2}\cos\frac{\phi}{2}z(t)\end{bmatrix} \tag{11}$$

with p being the frequency parameter, which for rectangular columns is equal with $p=\sqrt{3g/4R}$, and $\gamma_m=m_{BC}/2m_{AB}$ is the mass ratio.

3 SEISMIC PERFORMANCE OF THE HYBRID (FSHB) ROCKING BRIDGE BENT

This section investigates the seismic performance of the freestanding and hybrid FSHB rocking frame. Consider a cap-beam $13m$ wide, and $2m$ high. The frame consists of two square columns with $2b$=1.4m base length and $2H$=9.8m height, while the distance between the columns is L=8m (Fig. 1). The cap-beam-column mass ratio (γ_m) is considered as 5. The present analysis ignores (i) the deformation of the structural members, (ii) sliding between the contacting bodies and (iii) 3D rocking, and it focuses on the planar rocking motion of the frame.

3.1 Pulse-Type Ground Motions

To assess the seismic behaviour of the examined rocking frames, this section considers first pulse-type ground motions. Acceleration or velocity pulses often characterize strong ground motions near the fault of major earthquakes. Various mathematical expressions have been proposed to capture the long distinct pulses of near-fault ground motions (Voyagaki et al. (2013) among others). This study adopts the Mavroeidis and Papageorgiou (2003) (M&P) wavelet, which is described by four parameters that can idealize a wide range of near-fault ground excitations: (i) the frequency of the pulse (ω_g), (ii) the amplitude (α_g), (iii) the number (γ_g) and (iv) the phase angle (ν_g) of the half cycles. Eq. (12) provides the ground velocity of the M&P pulse, where parameter A controls the amplitude of the signal.

$$\begin{cases}\dot{u}_g(t)=-\frac{A}{2}\left[1+\cos\left(\frac{\omega_g}{\gamma_g}(t-t_0)\right)\right]\cos\left[\omega_p(t-t_0)+\nu_g\right], & t_0-\frac{\pi\gamma_g}{\omega_g}\le t\le t_0+\frac{\pi\gamma_g}{\omega_g}\\ 0 & ,otherwise\end{cases} \tag{12}$$

Fig. 3 compares the performance of the hybrid FSHB rocking frame (enhanced with elastic central tendons and hysteretic buckling restrained braces) with the pertinent freestanding frame. In particular, it examines structural systems, with different overall lateral stiffness (i.e. negative, zero and positive) for three levels of rocking rotation ($\phi_{\max}/\alpha=0.1,0.5,1.0$). In general, as the lateral stiffness increases, the seismic performance of the hybrid FSHB rocking frame is slightly enhanced compared to the freestanding frame. The improvement of the seismic behaviour of the hybrid frame is more evident for large rocking rotations ($\phi/\alpha=1.0$) and for small-sized columns (i.e. for $\alpha_g/g\tan\alpha=1$ to 3 and $\omega_g/p=1$ to 3). On the contrary, as the size of the columns (or the frequency of the excitation) increases, the hybrid frame's behaviour converges to that of the freestanding frame. Especially for

small rocking rotations ($\phi/\alpha = 0.1$), the two frames show almost identical stability results. Fig. 3 also verifies the beneficial effect of the dissipator's stiffness (ρ_d) increase, as it slightly enhances the frame's seismic performance regardless of the sign of the overall lateral stiffness.

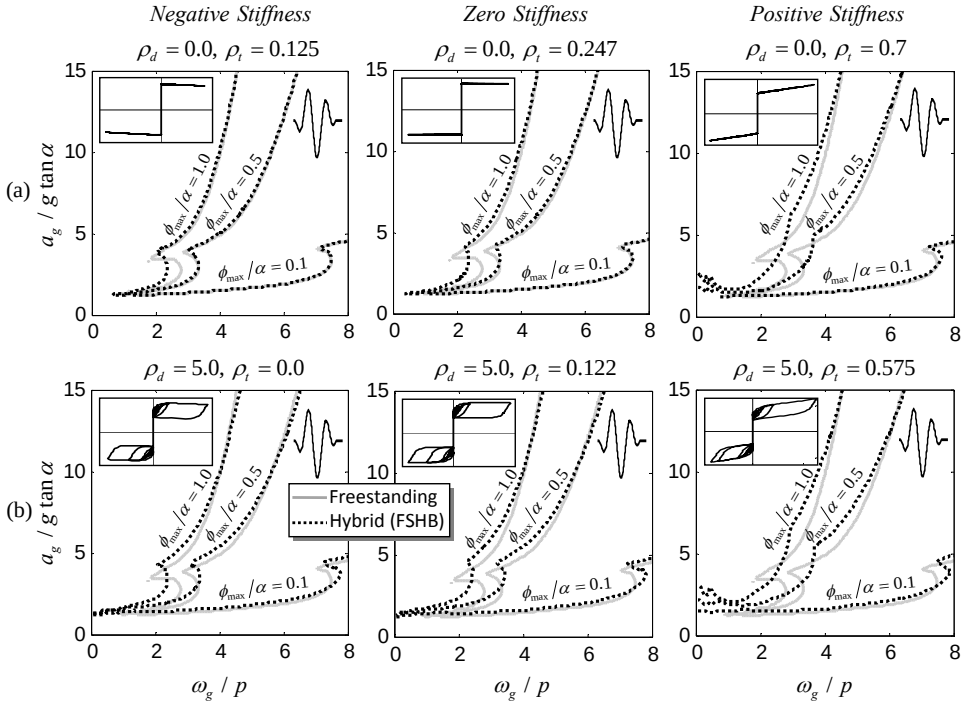

Fig. 3 Seismic performance of the rocking frame with u_y=3.5 mm subjected to M&P pulse (v_g=45° and γ_g=2.0) for the following dissipation parameters: (a) ρ_d=0.0 and (b) ρ_d=5.0

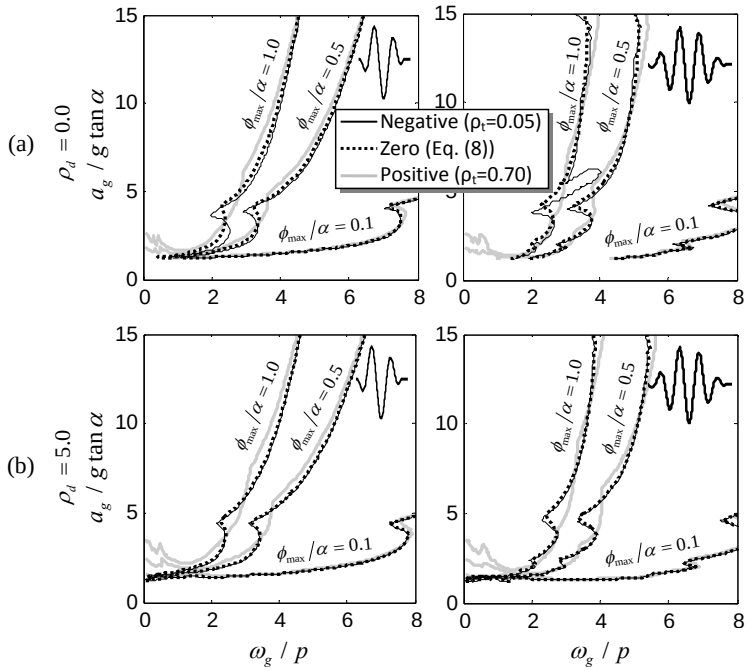

Fig. 4 Contour plots of the hybrid rocking frame with u_y=3.5 mm subjected to M&P pulse (v_g=0°, γ_g=2.0 (left) and γ_g=4.0 (right)), for the following dissipation parameters (a) ρ_d=0.0 and (b) ρ_d=5.0

Fig. 4 compares hybrid FSHB rocking frames with different post-uplift lateral stiffness (i.e. negative,

zero, positive). It also illustrates the effect on the seismic performance of increasing the number of the half-cycles (γ_g) of the ground excitation. Again, three levels of rocking rotation and two of the dimensionless parameter ρ_d are considered. In particular, Fig. 4 illustrates the relatively marginal enhancement of the seismic performance as the stiffness of the system increases. The comparison of the negative, zero and positive stiffness systems shows small differences in general, without any of the systems dominating the other two.

3.2 **Historic Excitations**

The present section extends the seismic analysis of the frame adopting historic earthquake records (Table 1), regardless of whether they contain distinguishable pulses or not. In particular, it employs a well-known set of historic ground excitations scaled to yield a probability of exceedance of 2% in 50 years (SAC 1997).

Table 1 Earthquake records (probability of exceedance of 2% in 50 years) (adapted from (SAC 1997))

Number	Record	Magnitude	Scale Factor	DT (s)	Duration (s)	PGA (cm/sec^2)
SE21	1992 Mendocino	7.1	0.98	0.02	59.98	741.13
SE22	1992 Mendocino	7.1	0.98	0.02	59.98	476.22
SE23	1992 Erzincan	6.7	1.27	0.005	20.775	593.60
SE24	1992 Erzincan	6.7	1.27	0.005	20.775	529.06
SE25	1949 Olympia	6.5	4.35	0.02	79.98	878.23
SE26	1949 Olympia	6.5	4.35	0.02	79.98	805.68
SE27	1965 Seattle	7.1	10.04	0.02	81.82	1722.40
SE28	1965 Seattle	7.1	10.04	0.02	81.82	1364.70
SE29	1985 Valpariso	8.0	2.9	0.025	99.975	1605.50
SE30	1985 Valpariso	8.0	2.9	0.025	99.975	1543.50
SE31	1985 Valpariso	8.0	3.96	0.025	99.975	1246.20
SE32	1985 Valpariso	8.0	3.96	0.025	99.975	884.43
SE35	1978 Miyagi-oki	7.4	1.78	0.02	79.98	595.07
SE36	1978 Miyagi-oki	7.4	1.78	0.02	79.98	768.62

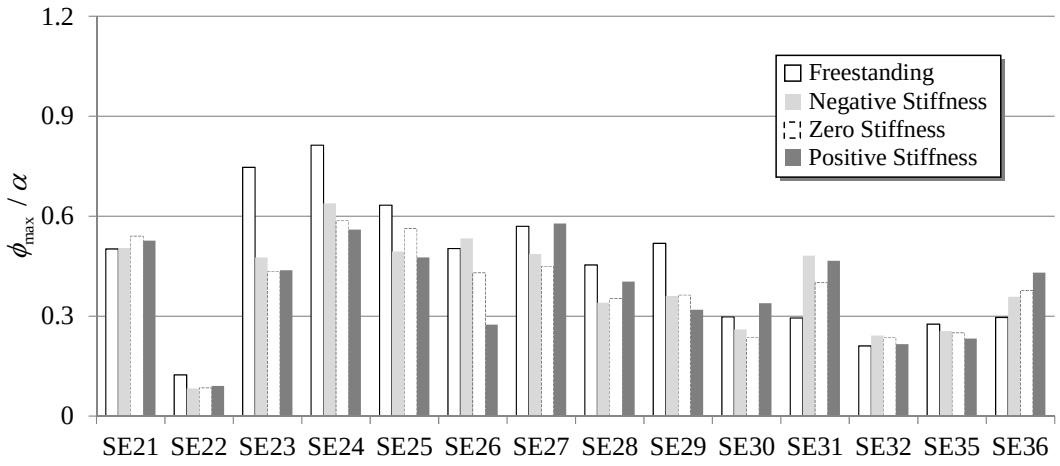

Fig. 5 Maximum rotations (in dimensionless terms) for all the earthquake records of Table 1

Fig. 5 and Fig. 6 compare the response of the freestanding with the pertinent hybrid FSHB rocking frame in terms of peak response and time history analysis respectively. Fig. 5 shows that although the earthquake records are scaled to the maximum credible earthquake level, both the freestanding and the hybrid FSHB rocking frame survive all the excitations. Recall that, according to the assumptions of the present study, when the examined frame survives the excitation, it eventually re-centers with no residual displacements/damage.

Further, Fig. 5 unveils the sensitivity of the freestanding rocking frame to the SE23, SE24 (Erzincan, Turkey) earthquake records. This is attributed to the distinguishable pulse these records contain. Recall that, large rocking structures (e.g. bridge bents) are particularly vulnerable to coherent ground motions (Acikgoz and DeJong 2014). Interestingly, for excitations without dominant distinguishable pulses (e.g. SE27, SE28) the response of the positive stiffness system is increased compared to the negative and the zero stiffness system. Note that, depending on the particular earthquake record examined, a different system performs the best (e.g. for SE31, SE36 the freestanding frame shows the best behaviour, while for SE28 the negative stiffness, for SE27, SE30 the zero stiffness and for SE25, SE26, SE29 the positive stiffness frame) (see also Fig. 6). Hence, the assessment of the seismic performance of the hybrid FSHB rocking frame beckons for a probabilistic evaluation (Dimitrakopoulos and Paraskeva 2015).

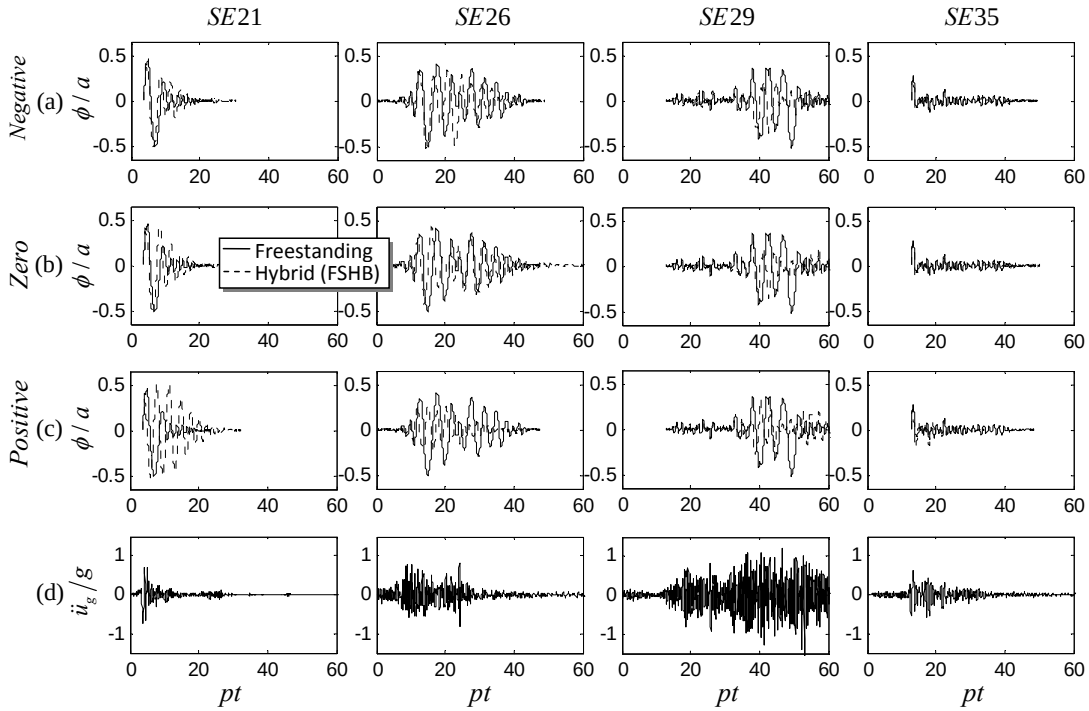

Fig. 6 Time history analyses for the hybrid rocking frame with u_y=3.5 mm and (a) negative, (b) zero (c) positive overall lateral stiffness under (d) different earthquake records

4 CONCLUSIONS

This study investigates the seismic performance of a planar freestanding and hybrid rocking frame (enhanced with additional energy dissipation and re-centering devices exhibiting flag-shaped hysteretic behaviour). The analysis quantifies the enhancement of the seismic performance of the hybrid FSHB frame as the overall lateral stiffness of the structure increases. However, this enhancement is marginal among the different stiffness systems examined. Further, this work reveals that depending on the particular earthquake record, and its characteristics (e.g. whether the record contains in its velocity or acceleration time-history a distinguishable pulse or not, the number of the excitation cycles etc.), a different rocking design solution (e.g. freestanding, hybrid with negative/zero/positive stiffness) might be better in terms of stability.

REFERENCES

Acikgoz, S. & DeJong, M. J. 2014. The rocking response of large flexible structures to earthquakes. *Bulletin of earthquake engineering.* 12(2). 875-908.

Black, C. J., Makris, N. & Aiken, I. D. 2004. Component testing, seismic evaluation and characterization of buckling-restrained braces. *Journal of Structural Engineering.* 130(6). 880-894.

Bouc, R. Forced vibration of mechanical systems with hysteresis. Proceedings of the fourth conference on non-linear oscillation, Prague, Czechoslovakia, 1967.

DeJong, M. J. & Dimitrakopoulos, E. G. 2014. Dynamically equivalent rocking structures. *Earthquake Engineering & Structural Dynamics.* 43(10). 1543-1563.

Dimitrakopoulos, E. G. & Giouvanidis, A. I. 2015. Seismic Response Analysis of the Planar Rocking Frame. *Journal of Engineering Mechanics.* 141(7). 04015003.

Dimitrakopoulos, E. G. & Paraskeva, T. S. 2015. Dimensionless fragility curves for rocking response to near-fault excitations. *Earthquake Engineering & Structural Dynamics.* DOI: 10.1002/eqe.2571.

Eatherton, M. R. & Hajjar, J. F. 2011. Residual drifts of self-centering systems including effects of ambient building resistance. *Earthquake Spectra.* 27(3). 719-744.

Housner, G. W. 1963. The behavior of inverted pendulum structures during earthquakes. *Bulletin of the Seismological Society of America.* 53(2). 403-417.

Kam, W. Y., Pampanin, S., Palermo, A. & Carr, A. J. 2010. Self-centering structural systems with combination of hysteretic and viscous energy dissipations. *Earthquake Engineering & Structural Dynamics.* 39(10). 1083-1108.

Kirkpatrick, P. 1927. Seismic measurements by the overthrow of columns. *Bulletin of the Seismological Society of America.* 17(2). 95-109.

Makris, N. & Vassiliou, M. F. 2012. Planar rocking response and stability analysis of an array of free-standing columns capped with a freely supported rigid beam. *Earthquake Engineering & Structural Dynamics.* 42(3). 431-449.

Makris, N. & Vassiliou, M. F. 2014. Dynamics of the Rocking Frame with Vertical Restrainers. *Journal of Structural Engineering.* 04014245.

Mander, J. B. & Cheng, C.-T. 1997. Seismic resistance of bridge piers based on damage avoidance design. *Technical Report: NCEER-97-0014.* University at Buffalo.

Marriott, D., Pampanin, S. & Palermo, A. 2009. Quasi-static and pseudo-dynamic testing of unbonded post-tensioned rocking bridge piers with external replaceable dissipaters. *Earthquake Engineering & Structural Dynamics.* 38(3). 331-354.

Mavroeidis, G. P. & Papageorgiou, A. S. 2003. A mathematical representation of near-fault ground motions. *Bulletin of the Seismological Society of America.* 93(3). 1099-1131.

Palermo, A., Pampanin, S. & Calvi, G. M. 2005. Concept and development of hybrid solutions for seismic resistant bridge systems. *Journal of Earthquake Engineering.* 9(06). 899-921.

Palermo, A., Pampanin, S. & Marriott, D. 2007. Design, modeling, and experimental response of seismic resistant bridge piers with posttensioned dissipating connections. *Journal of Structural Engineering.* 133(11). 1648-1661.

Pollino, M. & Bruneau, M. 2007. Seismic retrofit of bridge steel truss piers using a controlled rocking approach. *Journal of Bridge Engineering.* 12(5). 600-610.

SAC. 1997. *Suites of Earthquake Ground Motions* [Online]. Structural Engineers Association of California (SEA), Applied Technology Council (ATC) and Consortium of Universities for Research in Earthquake Engineering (CUREE). Available: http://nisee.berkeley.edu/data/strong_motion/sacsteel/ground_motions.html [Accessed 10 January 2014].

Voyagaki, E., Psycharis, I. N. & Mylonakis, G. 2013. Rocking response and overturning criteria for free standing rigid blocks to single—lobe pulses. *Soil Dynamics and Earthquake Engineering.* 46(85-95).

Wen, Y.-K. 1976. Method for random vibration of hysteretic systems. *Journal of the engineering mechanics division.* 102(2). 249-263.

Wiebe, L. & Christopoulos, C. 2014. Performance-based seismic design of controlled rocking steel braced frames. I: Methodological framework and design of base rocking joint. *Journal of Structural Engineering.* 141(9). 04014226.

Yim, C.-S., Chopra, A. K. & Penzien, J. 1980. Rocking response of rigid blocks to earthquakes. *Earthquake Engineering and Structural Dynamics.* 8(6). 565-587.